Study of Thermal Conductivity of PEM Fuel Cell Catalyst Layers

Odne S. Burheim[a,*], Huaneng Su[c,**], Hans Henrik Hauge[b], Sivakumar Pasupathi[c], Bruno Pollet[c]

[a]*Department of Electrical and Computational Engineering, HiST - Sor-Trondelag University College*

[b]*Department of Chemistry, Norwegian University of Science and Technology, 7491 Trondheim, Norway*

[c]*South African Institute for Advanced Materials Chemistry (SAIAMC), Faculty of Natural Sciences, University of the Western Cape, Cape Town, South Africa*

Abstract

In this study thermal conductivities of Polymer Electrolyte Membrane Fuel Cell (PEMFC) Catalyst Layers (CLs) were measured. The CLs were fabricated on a thin copper metal film, varied in composition and measured both when dry and in the presence of residual water. In order to demonstrate and evaluate the impact and relevance of the measurements, a 1-D thermal model was developed.

It was found that dry CLs, and CLs containing very small water content, had thermal conductivity values of 0.07-0.11 W K^{-1} m^{-1} when compressed in the range of 5-15 bar compaction pressure. When adding water up to 70 moles of water per mole of sulphonic group, it was observed that the water only had an effect on the thermal conductivity with values much higher than those reported as the capacity of the ionomer. The literature suggests, depending on the CL, that the ionomer of a CL can carry up to around 10 moles of water per sulphonic group and that water content beyond this level is carried otherwise. We found that for water content beyond 20 moles water per sulphonic group increases the thermal conductivity of the CL considerably. Thus water that is not kept by the ionomer contribute to the increased effective thermal conductivity of the CL while the water kept by of the ionomer has no impact. Absolute values of the thermal conductivity of the wetted "super saturated" CLs were not possible to determine due to the statistical noise in these experiments. The CLs were all found to compress irreversibly and to become incompressible above 10 bar compaction pressure

When considering wet porous transport layers (PTL) and moderately humidified CL, the PEMFC maximum internal temperature difference increased by 33% when compared to the commonly assumed measured thermal conductivities. Considering that the CL constitute less than 10% of the total PEMFC thickness

---

*Corresponding author; measurements and modelling.
**Corresponding author; catalyst layer sample preparation and development.
Email addresses: odnesb@hist.no (Odne S. Burheim), suhuaneng@gmail.com (Huaneng Su)

1. Introduction

Hydrogen is the fuel with the highest available gravimetric energy density. It is also a fuel that can be processed from almost any other energy sources. Currently, the most efficient and dynamic technology to convert the free energy of the hydrogen-oxygen chemical reactions is the low temperature Polymer Electrolyte Membrane Fuel Cell (PEMFC). When considering automotive applications; thermal management, degradation (ageing), and cost reductions are important factors for commercial deployment and success. A PEMFC is made of several important components, *i.e.* the Membrane Electrolyte Assembly (MEA) sandwiched between a thin Micro Porous Layer (MPL) and a somewhat thicker Porous Transport Layer (PTL). The MEA, in turn, consists of a membrane coated with catalyst layers, CL, on each side (Figure 1). In this paper we present for the first time, separate measurements of the thermal conductivity of the catalyst layer and compare it to thermal conductivities of other PEMFC components.

1.1. The role of the CL in a PEMFC

The CL, which is bound on one side by the gas diffusion layer (GDL) and on the other side by the Polymer Electrolyte Membrane (PEM), is the most active layer in an MEA of complex functionalities. It is a three-dimensional (3-D) porous structure composed of a network of catalyst nanoparticles and ionomer fragments. It is the layer where the electrochemical reactions take place, providing pathways for the transport of electrons, protons, reactants and products while facilitating Hydrogen Oxidation Reaction (HOR) at the anode and the Oxygen Reduction Reaction (ORR) at the cathode.

With respect to the importance of achieving high performance of PEMFC, extensive work has been performed to examine how the CL properties such as (i) the structure, (ii) the catalyst loading, and (iii) the ionomer content affect the fuel cell performance [1–4]. In contrast to that, the literature describing how the CL properties affect the heat management in the PEMFC is limited [5, 6], while this is very important

for real fuel cell applications [7] because the degradation of the ionomer, carbon supports and platinum nanoparticles is strongly associated with the temperature variations in the CL [8–10].

1.2. Measured Thermal Conductivity Measurements of PEMFC Components

Reliable measurements of the thermal conductivity of PEMFC materials is important and at the same time challenging. The water content, compaction pressure and temperature will change during PEMFC operation. Moreover, the PEMFC layer components are very thin with some of them being partially transparent. For some of the materials, the thermal conductivity is also non-isotropic. The challenges are different for each material and we present herein a short review of previous efforts in obtaining the thermal conductivity of the PEMFC component.

Based upon the available literature, it is fairly safe to say that the thermal conductivity of the PTL is now becoming well understood. The most thorough review available on this topic is, to our knowledge, one by Zamel and Li [11].

For the PTL, the in-plane and through-plane thermal conductivities are different. Because the in-plane electric conductivity is several times larger than the through-plane electrical conductivity, it was first postulated [12–14] and later verified experimentally [15–17] that the in-plane thermal conductivities are several times larger than the through-plane ones. It was found that the in-plane thermal conductivities are five to ten times larger than the through-plane ones (mainly depending on the PTL compaction).

In through-plane thermal conductivity measurements, the thermal contact resistance, the bulk material thermal conductivity and the thickness change with the applied compaction pressure must be accounted for [18–20]. In these measurements, one must separate the thermal contact resistance from the bulk material thermal resistance, which can lead to difficulties and reasonable assumptions must be made and accounted for. Both water and PolyTetraFluorEthylene (PTFE) will affect the thermal conductivity of the PTL [19–23].

First, the thermal conductivity was measured *in-situ* in the fuel cells by embedding thermocouples between the MPL and the catalyst layers and determining the thermal conductivity form the heat sources, see Vie and Kjelstrup [24]. The lack of precise knowledge of the location for the thermocouples reduced the precision with this approach. The first *ex-situ* experiments of thermal resistance (of the sample and the contact to the apparatus) were reported by Ihonen et al. [25]. Khandelwal and Mench [22] reported the first *ex-situ* measurements of PTL materials where the thermal conductivity and the thermal contact resistance to the

3

apparatus was de-convoluted. In this study [22], the compression, and thus the actual thickness, was not measured and hence the precision of the reported values decreased. Ramousse et al. [26] used a similar approach. The first report on *ex-situ* measurements accounting all of the three parameters required by Fourier's law and as a function of compaction pressures was that of Burheim et al. [19]. When correcting for the actual thickness due to the compression, the reported thermal conductivity values change by 5-20%. Perhaps the most important part of this study was that we demonstrated that the PTL-PTL contact thermal resistance is negligible and that therefore neglecting this when stacking materials is a valid approach for through-plane thermal conductivity measurements. Generally, these studies together suggested and agreed that at room temperature for dry materials the through-plane thermal conductivity of an ELAT PTL is around 0.2 W K^{-1} m^{-1}, a Sigracet PTL 0.3-0.4 W K-1 m-1 and Toray PTL is 0.3-0.8 W K-1 m-1.

Changes in temperature lead to changes in thermal conductivity for PTLs. These were measured both for in- and through-plane thermal conductivity by Zamel et al. [17, 27]. For the through-plane thermal conductivity with thickness controlled compression; it was found that at 16% compression (unknown compaction pressure) the thermal conductivity of the PTL, regardless of PTFE content, does not depend significantly on temperature [27]. For the in-plane thermal conductivity, it was found that for PTFE free PTLs the thermal conductivity is lowered by $\sim$ 50% when comparing values measured at room temperature to values from measurements undertaken at 60 °C and higher [17]. For the PTFE treated samples, the in-plane thermal conductivity is nearly unaffected in the range of -20 to +120 °C, respectively [17]. This is similar to what Khandelwal and Mench reported for Nafion$^{®}$ [22].

Adding water to the PTL has been measured to increase the thermal conductivity of every type of PTL at room temperature by a factor between two and three [20]. A recent study shows that the thermal conductivity increases gradually with the water content [28]. Moreover, this study shows that this effect is appears the strongest as water first enter the PTL and then level out as the pores are filled with water. The absence of a linear behaviour was previously shown [20], but never quantified like this [28]. At elevated temperatures, i.e. temperatures above 70 °C, the effective thermal conductivity is increased further by the so called heat pipe effect. The heat pipe effect is found to increase the through-plane thermal conductivity by 20-40%. [21].

PTFE is, on the contrary to water, found to decrease the through-plane thermal conductivity of every type of PTL. This is a common conclusion among all studies that includes varying the PTFE content. The common

understanding in the literature appears to be that under the absence of PTFE and when a PTL is compressed, more "fibre-to-fibre" contacts are produced leading to an increase of the effective thermal conductivity. In the presence of PTFE the uncompressed thermal conductivity of a PTL is increased by PTFE conducting some heat between the carbon fibres [29]. As soon as the PTL is compressed, the PTFE only inhibits more fibre to fibre contacts and then the effective through-plane thermal conductivity of the PTL is lowered in the presence of PTFE. This is observed even as the smallest portions of PTFE is added to the PTL.

Aged PTLs have reduced PTFE content. It has been shown that heat and water together remove some of the PTFE in the PTL. However an effect for the thermal conductivity is absent for the PTL dry thermal conductivity while the PTL becomes more susceptible to water when aged. Thus, the PTFE appear to be removed only at the locations away from fibre-to-fibre contact such that the thermal conductivity of the dry PTL remains unaffected and that the material still take up more water [30].

For Nafion$^®$, the PEMFC most commonly used membrane, there exists two studies on thermal conductivity. One shows that the thermal conductivity at room temperature increases linearly with water uptake, from 0.18 to 0.27 W K^{-1} m^{-1} at water content of close to 0 and up to 22 water per sulphonic group [19]. Another study showed that the thermal conductivity of a dry Nafion$^®$ increases linearly with temperature, from 0.17 to 0.14 at room temperature and 65 °C [22].

The thermal conductivity of different MPL made for PEMFC were, to our knowledge, for the first time investigated independently of any other fuel cell components [31]. The value was found to vary between 0.06 and 0.10 W K^{-1} m^{-1} at compaction pressures around 5 and 16 bar. Despite that the MPL are among the thinnest layers of a PEMFC they appear with a thermal conductivity so low that they can still have an important effect on the overall temperature distribution in a PEMFC. A recent study by Thomas et al. showed that the temperature gradient across this layer contribute to water transport and also that this increase in temperature helps keeping the water in the MPL in a gas phase [32]. The MPL and the catalyst layers have many similarities and therefore it is interesting to investigate the thermal conductivity also of the CL. In this study we show that the thermal and mechanical properties of CL are very similar to that of the MPL and that these layers thus are far from isothermal in an operating PEMFC.

1.3. Water Content

Thermal conductivity in PEMFC membrane and PTL materials has for long been known to be related to water content [19, 20]. For the perfluorosulfonate membrane, Nafion®, one typically gives the water content as number of water molecules per sulphonic group [33, 34]. This water content value is very often labelled λ and depends on the surrounding state of water. In this study we refer to the water content in this way, *i.e.* λ is moles of water per sulphonic group.

Moreover, the water content of surroundings can refer to the relative humidity in the ambient gas phase or it can be liquid water. Standard membrane preparation (heating the membrane to 90 °C in an oxidising acidic aqueous solution) leads to the membrane having a water content of around 0.5 when in dry conditions, 12-14 when exposed to water saturated gas (100% humidity) and around 22 when exposed to liquid water [33, 34]. According to equilibrium thermodynamics, water in saturated gas is in equilibrium with liquid water and hence it is expected that the water content is the same regardless of whether the water was in saturated gas phase or liquid water. However, this is not the case and this is known for many materials which is generally named the Schroedinger paradox. What is interesting, is that if the membrane is *not* treated with heated acidic oxidizing aqueous solutions, the Schroedinger paradox is no longer observed, and this is known as the absence of the Schroedinger paradox [35]. In the absence of the Schroedinger paradox, the membrane never obtain λ values above 14.

When the membrane becomes thinner the water content and proton conductivity also changes [36]. Clearly, care must be taken when considering the water content in the membrane material. Also, when the membrane is included in the catalyst layer the well established story about Nafion® and water content is different [37, 38]. When it comes to the water content in the catalyst layer, the Nafion® material will take up water linearly with relative vapour saturation up to 4-6 water molecules per sulphonic group. This is similar to what is seen in terms of additional absorption enthalpy of water in Nafion® [39]. Reucroft et al. showed that based on adsorption enthalpy of water, that water content above 5-6 in a Nafion® membrane relates to water-to-water interaction rather than water-to-sulphonic group interaction. In this context, it seems that water from a gas phase and in a catalyst layer will adsorb only to the sulphonic group water complex group and not to the ionomer back bone - which is reasonable considering the back bones similarities to PTFE. Another argument for this adsorption mechanism being reasonable for very thin ionomer films is that the activation energy for proton transport increases dramatically when the bulk membrane is made so thin that

6

it becomes a long chain with active sites rather than a bulk material[1], as observed by Paul et al. [36]. In this transition, the liquid water phase between the active cites, i.e. sulphonic groups, is repelled by the PTFE-like backbone. Water up-take to the ionomer in a CL from a liquid phase is, to our knowledge, not reported for CLs, possibly because one easily loose control of the water content as liquid water fill up pores of the catalyst carbon particles. However, if extrapolating the Schroeder paradox in the light of reported water content of CL, one can expect an increase of up to 50% in the water content when the CL is exposed to liquid water, *i.e.* a water content up to 9. However, considering that in a bulk membrane water is carried as little reservoirs and that we have neither treated the CL with nearly boiling acid nor have a bulk phase, we consider the Schroedinger paradox absent for the CL as deployed in this study. Hence, if we, in this study, report λ values above the value of 6, the remaining (above 6) will then be considered allocated otherwise than to the sulphonic group inside the CL.

2. Procedures

2.1. Thermal conductivity measurements

The measurement procedure is the exact same as the one in our previous paper on thermal conductivities in MPLs [30], and we refer to this paper for a more detailed explanation. The apparatus used in the experiments is depicted in Fig. 2. In brief, we measure the heat passing through the rig from top to bottom, q_i, along with the temperature difference across the sample, $T_4 - T_5$, as shown in Eq. 1 - 2. This gives us the thermal resistance of the investigated sample, R_{Sample}. The sample can be a stack of materials or a single layer. Here, we measure the sum of the sample stack and the contact thermal resistance to the machine surface, $R_{Sample}+2R_{App.-Sample}$. The stacks consist of layers of CL sandwiched between thin copper and aluminium films. One needs to subtract for the thickness of these metal films as they have negligible contribution to the thermal resistance, i.e. they only contribute to the thickness. Finally, we plot the thermal resistance as a function of the CL thickness and obtain the thermal conductivity from the inverse of the value

---

[1]Stricly speaking; Nafion® bulk material absorb water, sulphonic sites adsorb water and the CL containing sulphonic sites absorb water

of the slope.

$$q_{upper} = k_{steel}\frac{T_1 - T_3}{\delta_{1-3}} \ \text{ and } \ q_{lower} = k_{steel}\frac{T_6 - T_8}{\delta_{6-8}} \tag{1}$$

$$q_{Sample} = \frac{q_{upper} + q_{lower}}{2}, \ \text{ and; } \ R_{Sample} + 2R_{App.-Sample} = \frac{T_4 - T_5}{q_{Sample}} \tag{2}$$

Figure 2

2.2. CL preparation

For this study three types of catalyst layers were prepared - each in two different thickness'. These layers consisted of: 1) carbon black and ionomer equally in weight, 2) carbon black with 20wt% Pt and ionomer in equal weights, and 3) carbon black with 20 wt% Pt and twice as much ionomer in weight.

The CL were made by spraying a dispersion of the catalyst ink containing ionomer and catalyst particles onto one side of the copper foil (28 $\pm$2 μm, annealed, 99.8%, Alfa Aesar), followed by drying at 80 $^\circ$C (N$_2$ atmosphere) for 2 h to evaporate all remaining solvent (isopropanol).

The material was then overlaid with a thin pure aluminium foil and a circular punch was used to create discs that could be stacked on top of each other, in the same manner as in our paper on thermal conductivity of the MPL [30].

2.3. Statistical Analysis and Accuracy of the Measurements

The thermal conductivity apparatus was calibrated using materials with known thermal conductivity, see [19]. These values are known with 5% accuracy and thus this is the accuracy limitation of the reported values in this paper. Some of the results are reported with double standard deviations that are larger or smaller than 5% of the reported value. This is as the thermal conductivities are obtained by using a the linear regression in combination with a least square of residual approach. Hence the thermal conductivity variance reflects the fit on the line rather than the actual precision of the thermal conductivity.

When subtracting for the aluminium and copper film thickness the variances, $\sigma^2_{\delta_{Cu/Al}}$ will propagate and increase the CL thickness variance, $\sigma^2_{\delta_{CL}}$ as given by the equation of error propagation, Eq. 3. This, in

combination with the thickness calibration, is what gives the reported thickness double standard deviation, $2\sigma_{\delta_{sample}}$, reported along with the measured thermal resistance.

$$\sigma_i^2 = \sum_{n=1}^{i} \left(\frac{\partial f(x_1, x_2, ..., x_i)}{\partial x_n} \sigma_n \right)^2 \tag{3}$$

2.4. Temperature Distribution Model

Non-isothermal mathematical models have become more of a standard for PEMFCF over the past decade, see e.g. Bapat and Thynell [40] and by Zhang and Khandlikar [41]. In this paper we present a model that accounts for temperature gradients induced by standard heat sources in order to show the importance of the presented thermal conductivity values. With the objective of only demonstrating the effect of thermal conductivity in the CL we settle for a simple model as explained in the following paragraphs.

Table 1

The model is developed in the commercial software Comsol 4.2a which is set to solve

$$\nabla \left(k_i \nabla T \right) + \dot{Q}_i = 0 \tag{4}$$

where k_i is the thermal conductivity and $\dot{Q}_i$ is the volumetric heat source for region i as given in Table 1. The model was solved using Dirichlet boundary conditions at the sides and fixed temperatures at the end. This eventually leaves us with a one-dimensional model. The model was solved for using quadratic mesh and because of the second order polynomial behaviour one needs only one frame (mesh) per layer.

Figure 3

A linkage between the modelled area in this paper, a fuel cell sketch, and a SEM micrograph of two Freudenberg FFCT H2315 3X196 PTL coated with MPL sandwiching a custom made MEA (0.4 mg Pt cm^{-2} on a Nafion® 212) are given in Fig. 3. Typically, the PTL thickness is around one order of magnitude thicker than the rest of the PEMFC layers. In this model we chose the thickness of 255 μm (similar to a Toray TGP-090 at 13 bar compression) and that the PTL would contain some residual water. As discussed previously, the PTL is typically topped with a MPL that is partly integrated in the PTL an partly on top of the PTL [31]. The part of the MPL that is integrated with the PTL is considered to have the thermal properties of the PTL in this model while the MPL fraction on top is considered to have thermal properties of pure MPL - assumptions consistent with previous studies [30, 31]. Although the membrane in the SEM micrograph in Fig. 3 is a 2 mill thick Nafion®, we have chosen to include a somewhat thinner membrane in the model. This is as we

9

know from experience that it is much likelier for a commercial PEMFC to have a 30 μm thick membrane than one of 55 μm. Finally, to the catalyst layers. These layers constitute the main interest in this study, and based on the known thermal conductivities of the other layers in the PEMFC the reported values in this paper are very low. In fact their thermal conductivity are one order of magnitude less than that of some of the most widely applied PTL. We have chosen to apply four different values of thermal conductivity in this model. This is so that one can get an idea of the impact of using the values obtained in this study compared to studies using values similar to those of the commercial PTL with the highest thermal conductivities.

3. Results and Discussion

3.1. Thermal conductivity

The thermal conductivity was investigated for differently composed catalyst layers when dry and when humidified with water from a vapour phase. We separate the measurement results into two different subsections; one for the dry and and another for the wet materials.

Table 2

3.1.1. Dry Catalyst Layers

Figure 4

The thermal conductivity of the catalyst layers under various compaction pressure is listed in Table 2. The thermal conductivity is ranging from 0.04-0.08 W K^{-1} m^{-1} at 4.6 bar compaction pressure to 0.07-0.11 at 16.1 bar compaction pressure. When comparing to the thermal conductivity of air, 0.025 W K^{-1} m^{-1}, the thermal conductivity of this porous transport layer is very low. It is as high as four times that of air. The thermal conductivity of most porous carbon papers, PTL, used in fuel cells have a thermal conductivity in the range of 0.3-0.7 W K^{-1} m^{-1} (see the introduction), which is ten times larger than than what is observed for the catalyst layers in these measurements. However, if we compare these measurements to other electrochemical porous electrodes that are more similar to the CL than PTL, the reported thermal conductivity values are in good agreement. The thermal conductivity of such materials are; activated carbon mixed with 5 wt% PTFE for supercapacitors is around 0.13 W K^{-1} m^{-1} [42], activated carbon mixed with 10-25 wt% PTFE for PEMFC MPL is in the range 0.07-0.10 W K^{-1} m^{-1} [31], non-graphitised carbon cones with 5 wt% polyvinylidene flouride, PVDF, is around 0.07 W K^{-1} m^{-1} [43]. In this context, the values measured and reported here are reasonable.

Figure 5

10

The only parameter in this study that has a significant impact on thermal conductivity of dry CL is the compaction pressure. This can be seen from the results in Table 2. This can also be seen in Figure 4, where the thermal resistance of the catalyst layer containing no Pt is shown for increasing compaction pressures. At first sight, however, the thermal conductivity can appear to be affected by the presence of Pt in the catalyst nanoparticles. This is not significant however. The only effect that can be seen in relation to the Pt content is an enlarged uncertainty of the actual value of the thermal conductivity. This is due to the measured thermal resistance being more scattered for these series of measurements. This can be seen when comparing Fig. 5 to the results from 9.3 bar compaction pressure in Fig. 4. These three graph are fairly similar, again showing that the CL composition is of no significant importance to the thermal conductivity.

On the other hand and when studying these three graphs in greater detail, it can off course be tempting to try to relate the scatter of the results in Fig. 5 to our chosen method of stacking the samples and excluding the stack internal contact resistances. In particular when looking at the measurements obtained with a one-to-one catalyst-Nafion® mixture in Fig. 5, where the two thicker measurement points consist of two layers stacked and the two thinner sample are single layers. However, when attempting to account for this potential extra internal contact resistance by "linearising" the two thicker and the two thinner samples, we do not obtain a result significantly different from the results in Table 2. Moreover, the trend in this figure is neither seen in any other of our studies nor in our validation of the chosen procedure and considered a random error.

Figure 6

When studying the effect of compaction pressure, we turn to Fig. 6. For the three differently composed materials the trend is similar: The thermal conductivity is increased almost irreversibly and the thickness decreases entirely irreversibly. Moreover, theses changes appear much clearer during the first part of the compaction cycle. This effect can be seen in the light of compaction. That is; when these porous materials are compressed the thickness is reduced and the amount of contact points between the nanoparticles are increased. Correspondingly the thermal conductivity of the material as a whole increases. This increase can only occur up to the point when the material is fully compacted. From Fig. 4, 5, 6, and Table 2, the point of complete compaction appear to be at a compaction pressure of around 10 bar. This point is also the point when the thermal conductivity of similar materials appear to be independent of whether they are compressed as in our apparatus or machined by calendering [31, 42].

The subject of response to compaction is important for at least two reasons; one is the comparison between

materials compacted by different tools and the other is the response of a dynamic compaction stress in a real fuel cell system. The first point is discussed previously in this section when validating our results. In a fuel cell system, the compaction is dynamic in part from thermal hysteresis and in part form wetting expansion in a Nafion® membrane. The PTL used in a PEMFC system today is typically much more elastic [44] than the membrane [19], MPL [31] and CL (seen here) and will therefore take up all of the expansion that occurs during the life cycle of a PEMFC. This is important because it means that the only thermal conductivity reported in this section that is really relevant for real life applications are those values measured at compaction pressures above 10 bars.

The Nafion® content does not affect the thermal conductivity of the CL. This is perhaps surprising because it is well established by measurements and modelling (see the introduction) that PTFE impedes the heat transfer in PTL materials. This effect is known to appear from the point when PTFE is first introduced to the PTL materials and less so when more PTFE is added. Also for the MPL it is seen that changing the PTFE content from 10 to 25wt% does not change the thermal conductivity to any significant level. In this light it is not surprising that the thermal conductivity of the dry CL does not change significantly when doubling the Nafion® content.

3.1.2. Catalyst Layers with Water

Table 3

The presence of water is known to increase the thermal conductivity of the PTL [20, 21, 30] and the membrane of the PEMFC [19, 22]. Therefore we have also in this study included experiments where the investigated materials contain liquid water. It is generally known that that PTFE makes these types of measurements difficult and that when Nafion® is present as thin as in a CL it goes from being relatively hydrophilic to being relatively hydrophobic. Moreover, measuring PTL materials with water is to our experience challenging both in terms of obtaining a reproducible water content and also with respect to measure a thermal conductivity with high precision [20]. In this perspective we can only expect that the present study will obtain some qualitative results when it comes to determining the thermal conductivity of CLs containing liquid water.

Figure 7

In Table 3 we have summarised the measured thermal conductivities and the water content in each case. In general, neither the compaction pressure nor the catalyst content appear to be the principal component for the change in thermal conductivity of the CL containing liquid water. The Nafion® content, however,

12

appear to have an enormous impact on the reproducibility of the thermal resistance measurements. As long as the ratio between the carbon particle content and the Nafion® content is on a one-to-on level we have steady measurements and the thermal conductivity ranges from 0.10 to 0.15 W K^{-1} m^{-1} when the compaction pressure increase from 5 to 16 bars. A similar trend, i.e. increasing thermal conductivity with increasing compaction pressure, appears also for the CL with higher ionomer content, however not significant. Moreover, the value of the thermal conductivity appear to be much larger for the CL with higher ionomer content. As difficult it is to assess this value precisely, it is clear from the measured thermal resistance, see Fig. 8, that this material absorb much more water and that the thermal resistance is reduced much more than for the wet CL containing equal amounts of catalyst particles and ionomer.

Figure 8

We have chosen to represent the water content in terms of water molecules per sulphonic group, traditionally labeled λ. As mentioned in the introduction, values above 6 (or possibly 9 in the presence of the Schroedinger paradox) is not likely to be related to Nafion® however. When we report a content of e.g. 40, we consider that for every sulphonic group there are around 34 (or 31) water molecules in the CL that are not associated with the sulphonic group of the ionomer. This water can be trapped in pores of the CL particles or between the nanoparticles, thus contributing to an increase in the thermal conductivity. Looking carefully at Fig. 7 and 8 it seems as if there is a water content threshold for which the thermal specific resistance is significantly different from the dry CL. When the water content is less 25 we do not observe an impact on the measure thermal specific resistance. For the data points of the lower thickness this is difficult to argue because the measured thermal specific resistance is very low in both instances. For some of the thicker samples, however, this trend appear much more evident. In this study we did not have access to the equipment that could allow us to control the water content in detail. It is, nevertheless, an important observation to pursue in the future. This is as the state of water changes very rapidly and is very sensitive in the temperature range of 65-95 °C and that also the thermal conductivity clearly depends considerably on these conditions.

The subject of precisely how and where this residual water content is allocated is can not be determined based upon the present paper. What can be concluded, however, is that for the reproducible thermal resistance measurements; the thermal conductivity increases with around 50%. Moreover, this result is obtained with the maximum water content that we could obtain. Thus we have a lower and an upper boundary for what the thermal conductivity can be, i.e. for a CL containing equal masses of catalyst particles and

13

^{342} Nafion®, the thermal conductivity of dry material is at least 0.07 W K^{-1} m^{-1} and the upper limit for the

^{343} wet CL is 0.15 W K^{-1} m^{-1}.

3.2. Thermal modeling

^{345} As already mentioned, a one-dimensional thermal model of a PEMFC operated at 70 °C, +0.7 V and 1

^{346} A cm^{-2} was developed. In this model we changed the thermal conductivity of the CL from 0.07 to 0.7

^{347} W K^{-1} m^{-1}. The results are plotted in Fig. 9. When comparing the maximum temperature difference

^{348} in the model for thermal conductivities as high as those of wet PTL (0.7) to those obtained for the dry

^{349} CL thermal conductivity (0.07), the temperature difference increases by 33%. Even when comparing the

^{350} temperature increase for the wet PTL (0.07) and the wet CL (0.11), the increase is more than 20%. This

^{351} clearly demonstrates that the findings of this paper are important for the modellers and that more water

^{352} content research of the CL is indeed needed.

^{353} The model considers PTLs with a rather high thermal conductivity. This is due to the fact that under the

^{354} land of a bipolar plate, the PTL typically contains residual water [45]. Hence the relative increase of the

^{355} temperature difference value is maximised in this study. However, it is also well-known that under land is

^{356} the lowest current density in fuel cell that have parallel flow fields [12, 46, 47]. Since the current densisty

^{357} can be much larger under the gas flow channel and that this is the region with the highest current density, the

^{358} absolute temperature difference can be much larger than what we have shown with our model. As interesting

^{359} as it might be, studying this in greater detail is beyond the scope of this paper.

4. Conclusions

^{361} The thermal conductivity of catalyst layers (CL) for the PEMFC with different content of platinum and

^{362} Nafion® ionomer was measured at different compaction pressure and with different water content. CL with

^{363} little and moderate water content, thermal conductivity values were found to be in the range of 0.07-0.10

^{364} W K^{-1} m^{-1} when the pressure increased from around 5 to 15 bar compaction pressure. When allowing

^{365} water to condense onto the catlayst layers, the ionomer became over saturated with water and residual water

^{366} was found in the catalyst layers. For these "supersaturated" CLs the thermal conductivity value can be

^{367} expected to increase by 50% when the CL consists of equal amounts of Nafion® and catalyst nanoparticles.

^{368} Doubling the Nafion® ionomer content strengthened the effect of increased thermal conductivity when

super saturating the CLs. Accounting for the uncertainty, a threefold increase in thermal conductivity is not unlikely. The CLs were all found to compress almost irreversibly and to be hardly compressible beyond a compaction pressure of around 10 bar.

By deploying a one dimensional (1-D) model for an under-land region and 10 kA $^{-2}$ at +0.7 V, it was shown that the maximum temperature difference between the polarisation plates and the PEMFC increased by as much as 33% when considering moderately humidified CLs.

References

[1] Q. Wang, M. Eikerling, D. Song, Z. Liu, T. Navessin, Z. Xie, S. Holdcroft, Functionally graded cathode catalyst layers for polymer electrolyte fuel cells: I. theoretical modeling, Journal of The Electrochemical Society 151 (7) (2004) A950–A957.

[2] H.-N. Su, S.-J. Liao, Y.-N. Wu, Significant improvement in cathode performance for proton exchange membrane fuel cell by a novel double catalyst layer design, Journal of Power Sources 195 (2010) 3477 − 3480.

[3] A. Chaparro, B. Gallardo, M. Folgado, A. MartÃn, L. Daza, {PEMFC} electrode preparation by electrospray: Optimization of catalyst load and ionomer content, Catalysis Today 143 (3-4) (2009) 237 − 241.

[4] G. Sasikumar, J. Ihm, H. Ryu, Optimum nafion content in {PEM} fuel cell electrodes, Electrochimica Acta 50 (2 - 3) (2004) 601 − 605.

[5] A. Kulikovsky, Heat transport in a pefc: Exact solutions and a novel method for measuring thermal conductivities of the catalyst layers and membrane, Electrochemistry Communications 9 (1) (2007) 6 − 12.

[6] A. Kulikovsky, Thermal stability of the catalyst layer operation in a fuel cell, Journal of Electroanalytical Chemistry 652 (1 - 2) (2011) 66 − 70.

[7] W. Zhang, C.-w. Wu, Effect of clamping load on the performance of proton exchange membrane fuel cell stack and its optimization design: A review of modeling and experimental research, Journal of Fuel Cell Science and Technology 11 (2014) 021012–1–11.

[8] I. Tolj, D. Bezmalinovic, F. Barbir, Maintaining desired level of relative humidity throughout a fuel cell with spatially variable heat removal rates, International Journal of Hydrogen Energy 36 (20) (2011) 13105 – 13113.

[9] F. Barbir, I. Tolj, D. Bezmalinovic, Maintaining desired temperature and relative humidity throughout a fuel cell, ECS Transactions 41 (1) (2011) 1879–1886.

[10] J. D. Fairweather, D. Spernjak, A. Z. Weber, D. Harvey, S. Wessel, D. S. Hussey, D. L. Jacobson, K. Artyushkova, R. Mukundan, R. L. Borup, Effects of cathode corrosion on through-plane water transport in proton exchange membrane fuel cells, Journal of The Electrochemical Society 160 (9) (2013) F980–F993.

[11] N. Zamel, X. Li, Effective transport properties for polymer electrolyte membrane fuel cells – with a focus on the gas diffusion layer, Progress in Energy and Combustion Sci. 39 (2013) 146.

[12] J. Pharoah, K. Karan, W. Sun, On effective transport coefficients inPEM fuel cell electrodes: Anisotropy of the porous transport layer, J. Power Sources 161 (2006) 214–224.

[13] F. Danes, J. Bardon, Thermal conductivity of the carbon felts, strongly anisotropic insulants: Modelling of heat conduction by solid phase. Uses of carbon felts for high temperature insulation are reviewed. Effects of raw material and fabrication 36 (2008) 200–208.

[14] E. Sadeghi, M. Bahrami, N. Djilali, Analytic determination of the effective thermal conductivity of PEM fuel cell gas diffusion layers, J. Power Sources 179 (2008) 200–208.

[15] E. Sadeghi, N. Djilali, M. Bahrami, A novel approach to determine the in-plane thermal conductivity of gas diffusion layers in proton exchange membrane fuel cells, J. Power Sources 196 (2011) 3565–3571.

[16] P. Teertstra, G. Karimi, X. Li, Measurement of in-plane effective thermal conductivity in PEM fuel cell diffusion media, Electrochimica Acta In Press.

[17] N. Zamel, E. Litovsky, S. Shakhshir, X. Li, J. Kleiman, Measurement of in-plane thermal conductivity of carbon paper diffusion media in the temperature range of -20 °c to +120 °c, Appl. Energy 88 (2011) 3042–3050.

[18] J. Ramousse, O. Lottin, S. Didierjean, D. Maillet, Estimation of the thermal conductivity of carbon felts used as PEMFC gas diffusion layers, Int. J. of Thermal Sci. 47 (2008) 1–6.

[19] O. Burheim, P. Vie, J. Pharoah, S. Kjelstrup, *Ex-situ* measurements of through-plane thermal conductivities in a polymer electrolyte fuel cell, Journal of Power Sources 195 (2010) 249–256.

[20] O. Burheim, H. Lampert, J. Pharoah, P. Vie, S. Kjelstrup, Through-plane thermal conductivity of PEMFC porous transport layers, Journal of Fuel Cell Science and Technology 8 (2011) 021013–1–11.

[21] Y. Wang, M. Gundevia, Measurement of thermal conductivity and heat pipe effect in hydrophilic and hydrophobic carbon papers, Int. J. Heat Mass Transf. 60 (2013) 134–142.

[22] M. Khandelwal, M. M. Mench, Direct measurement of through-plane thermal conductivity and contact resistance in fuel cell materials, J. Power Sources 161 (2006) 1106–1115.

[23] H. Sadeghifar, N. Djilali, M. Bahrami, Effect of polytetrafluoroethylene (ptfe) and micro porous layer (mpl) on thermal conductivity of fuel cell gas diffusion layers: Modeling and experiments, Journal of Power Sources 248 (0) (2014) 632 – 641.

[24] P. Vie, S. Kjelstrup, Thermal conductivities from temperature profiles in the polymer electrolyte fuel cell, Electrochimica Acta 49 (2004) 1069–1077.

[25] J. Ihonen, M. Mikkola, G. Lindhberg, The flooding of gas diffusion backing in PEFCs; physical and electrochemical characterisation, J. Electrochem. Soc. 151 (2004) A1152–A1161.

[26] J. Ramousse, O. Lottin, S. Didierjean, D. Maillet, Heat sources in Proton Exchange Membrane (PEM) fuel cells, Journal of Power Sources 192 (2009) 435–441.

[27] N. Zamel, E. Litovsky, S. Shakhshir, X. Li, J. Kleiman, Measurement of the through-plane thermal conductivity of carbon paper diffusion media for the temperature range from -50 to +120 °c, Int. J. Hydrogen Energy 36 (2011) 12618–12625.

[28] G. Xu, J. M. LaManna, M. M. Mench, Direct measurement of through-plane thermal conductivity of partially saturated fuel cell diffusion media, J. Power Sources XXX (2014) In press.

[29] J. Yableckia, A. A. Nabovati, A. Bazylak, Modeling the effective thermal conductivity of an anisotropic gas diffusion layer in a polymer electrolyte membrane fuel cell, J. Electrochem. Soc. 159 (2012) B647–B653.

17

[30] O. S. Burheim, G. Ellila, J. D. Fairweather, A. Labouriau, S. Kjelstrup, J. G. Pharoah, Ageing and thermal conductivity of porous transport layers used for pem fuel cells, Journal of Power Sources 221 (2013) 356–365.

[31] O. S. Burheim, H. Su, S. Pasupathi, J. G. Pharoah, B. G. Pollet, Thermal conductivity and temperature profiles of the micro porous layers used for the polymer electrolyte membrane fuel cell, International Journal of Hydrogen Energy 38 (2013) 8437 – 8447.

[32] A. Thomas, G. Maranzana, S. Didierjean, J. Dillet, O. Lottin, Thermal and water transfer in pemfcs: Investigating the role of the microporuos layer, Int. J. of Hydrogen Energy XX (2014) XXX–XXX.

[33] T. A. Zawodzinski, M. Neeman, L. O. Sillerud, S. Gottesfeld, Determination of water diffusion coefficients in perfluorosulfonate ionomeric membranes, The Journal of Physical Chemistry 95 (15) (1991) 6040–6044.

[34] T. A. Zawodzinski, J. Davey, J. Valerio, S. Gottesfeld, The water content dependence of electro-osmotic drag in proton-conducting polymer electrolytes, Electrochimica Acta 40 (1995) 297 – 302.

[35] L. M. Onishi, J. M. Prausnitz, J. Newman, Water-nafion equilibria. absence of schroeder's paradox, The Journal of Physical Chemistry B 111 (34) (2007) 10166–10173.

[36] D. K. Paul, A. Fraser, K. Karan, Towards the understanding of proton conduction mechanism in {PEMFC} catalyst layer: Conductivity of adsorbed nafion films, Electrochemistry Communications 13 (8) (2011) 774 – 777.

[37] H. Iden, K. Sato, A. Ohma, K. Shinohara, Relationship among microstructure, ionomer property and proton transport in pseudo catalyst layers, J. Electrochem. Soc. 158 (2011) B987–B994.

[38] A. Kusoglu, A. Kwonga, K. T. Clark, H. P. Gunterman, A. Z. Weber, Water uptake of fuel-cell catalyst layers, J. Electrochem. Soc. 159 (2012) F530–F535.

[39] P. Reucroft, D. Rivin, N. Schneider, Thermodynamics of nafion-vapor interactions. I. Water vapor, Polymer 43 (2002) 5157–5161.

[40] C. Bapat, S. Thynell, Anisotropic heat conductions effects in proton-exchange membrane fuel cells, ASME, Journal of Heat Transfer 129 (2007) 1109–1118.

[41] G. Zhang, S. G. Kandlikar, A critical review of cooling techniques in protone exchange membrane fuel cell stacks, Int. J. Hydrogen Energy 37 (2012) 2412–2429.

[42] O. S. Burheim, M. Aslan, J. S. Atchison, V. Presser, Thermal conductivity and temperature profiles in carbon electrodes for supercapacitors, Journal of Power Sources 246 (2014) 160 – 166.

[43] O. S. Burheim, M. A. Onsrud, J. G. Pharoah, F. Vullum-Bruer, P. J. S. Vie, Thermal conductivity, heat sources and temperature profiles of li-ion secondary batteries, ECS Transactions – Submitted Dec. 6.

[44] E. Sadeghi, N. Djilali, M. Bahrami, Effective thermal conductivity and thermal contact resistance of gas diffusion layers in proton exchange membrane fuel cells. part 2: Hysteresis effect under cyclic compressive load, J. Power Sources 195 (2010) 8104–8109.

[45] A. Turhan, K. Heller, J. S. Brenizer, M. M. Mench, Passive control of liquid water storage and distribution in a pefc through flow-field design, Journal of Power Sources 180 (2008) 773 – 783.

[46] D. Harvey, J. Pharoah, K. Karan, J. Power Sources 179 (2008) 209–219.

[47] S. Reum, M. Freunberger, A. Wokaun, F. Buchi, J. Electrochem. Soc. 156 (2009) B301–B310.

Tables

Table 1: The model parameters used for the model in this paper.

Material	k / W K^{-1}m^{-1}	δ_i / μm	$\dot{Q}_i \cdot \delta_i$ / W m^{-2}
Backing	200	$\geq$100	–
Contact	0.7	5	–
PTL	0.96	255	–
MPL*	0.10	10	–
Anode	0.07, 0.11, 0.15, 0.7	10	$0.001\,j$
Cathode	0.07, 0.11, 0.15, 0.7	20	$\left(0.45 + 0.06\ln\frac{j}{10^4} + \frac{T\Delta S}{2F}\right)$ j
Membrane	0.25	30	$\frac{\delta_i}{8.7}j^2$

*Refers to MPL that is not integrated with the PTL.

Table 2: Measured thermal conductivities of the dry catalyst layers. Reported units are in mW K^{-1} m^{-1}.

Press. / bar	C:Nafion®=1:1, no Pt	C:Nafion®=1:1, 20wt% Pt/C	C:Nafion®=1:2, 20wt% Pt/C
4.6$^{\Uparrow}$	74 ± 10	63 ± 27	64 ± 14
9.2$^{\Uparrow}$	85 ± 9	69 ± 33	72 ± 20
13.8$^{\Uparrow}$	95 ± 5	76 ± 30	78 ± 21
16.1$^{\Uparrow}$	98 ± 8	78 ± 25	83 ± 24
4.6$^{\Downarrow}$	87 ± 5	71 ± 24	75 ± 21

Table 3: Thermal conductivity of differently composed and compressed catalyst layers that have absorbed water from condensing steam.

Press. / bar	C:Nafion®=1:1, no Pt	C:Nafion®=1:1, 20wt% Pt/C	C:Nafion®=1:1, 20wt% Pt/C
$4.6^{\Uparrow}$	0.10 ± 0.13	0.13 ± 0.04	0.2 ± 0.3
$9.2^{\Uparrow}$	0.13 ± 0.15	0.12 ± 0.02	0.3 ± 0.8
$13.8^{\Uparrow}$	0.15 ± 0.14	0.12 ± 0.02	0.4 ± 0.9
$16.1^{\Uparrow}$	0.14 ± 0.10	0.12 ± 0.02	0.5 ± 1.0
$4.6^{\Downarrow}$	0.12 ± 0.18	0.11 ± 0.02	0.4 ± 0.8
λ	70 ± 30	40 ± 40	70 ± 30

Figure Captions

Figure 1. Schematic diagram of a 7-layer structure MEA with MPL sandwiched between two PTL in turn between two polarisation plates.

Figure 2. A 2D sketch of the apparatus used to measure thermal conductivity as reported here. [30]
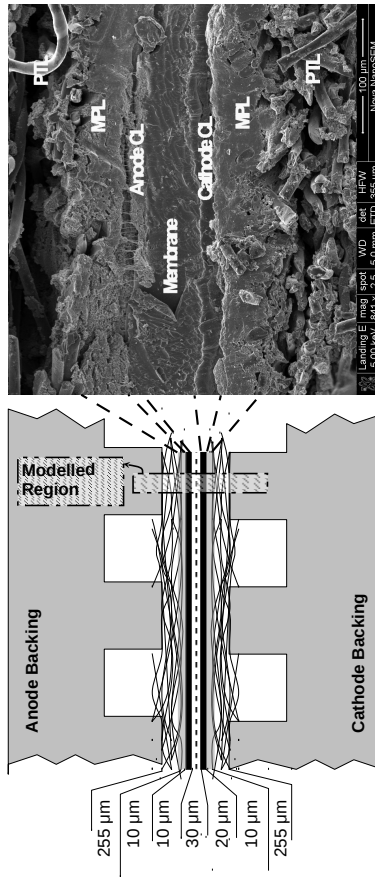
Figure 3. A SEM micrograph of a PEMFC MEA, MPL, and parts of PTL (top) and a PEMFC (bottom) illustrating the link to the chosen geometry in this study.
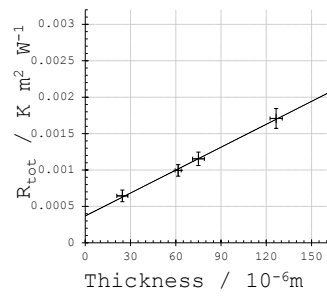
Figure 4. Measured thermal specific resistance for the CL containing no Pt catalyst and a Nafion$^{\circledR}$:carbon ratio of 1:1.

Figure 5. Measured thermal specific resistance for the CL where the carbon particles contain 20 wt% Pt at a compaction pressure of 9.3 bar.

Figure 6. Measured relative compression (left axes) and thermal conductivity (right axes) from around 4.6 bar compression and upwards to 16.1 bar and down again.

Figure 7. Measured thermal specific resistance for the CL containing no Pt catalyst and a Nafion$^{\circledR}$:carbon ratio of 1:1. The figure shows the results for the dry samples and the samples containing water. The water contents, λ, are indicated next to each data point.

Figure 8. Measured thermal specific resistance for the humidified CL at 9.3 bar compaction pressure, and with 20 wt%Pt on the carbon and different ionomer content. The water contents, λ, are indicated next to data point.

Figure 9. Modeled temperature profiles considered between the middle of two flow channel ribs.
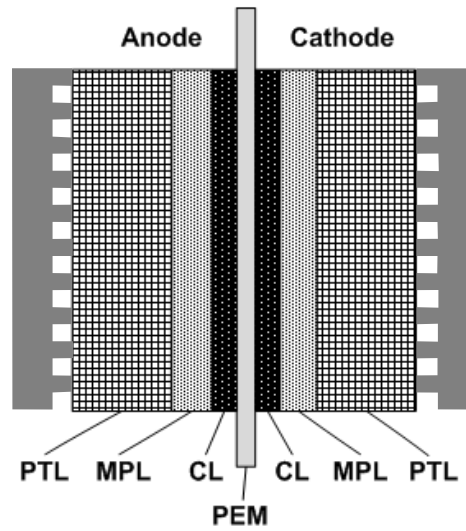
Figures

Figure 1: Schematic diagram of a 7-layer structure MEA with MPL sandwiched between two PTL in turn between two polarisation plates.
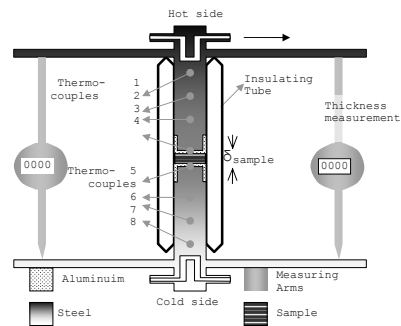
Figure 2: A 2D sketch of the apparatus used to measure thermal conductivity as reported here. [30]

Figure 3: A SEM micrograph of a PEMFC MEA, MPL, and parts of PTL (top) and a PEMFC (bottom) illustrating the link to the chosen geometry in this study.
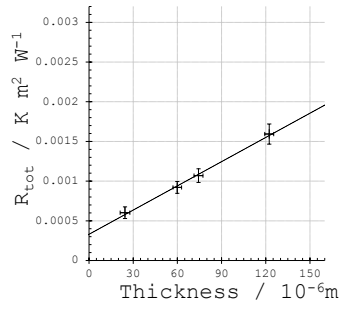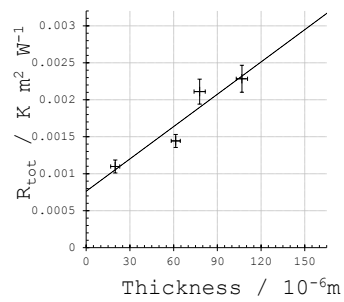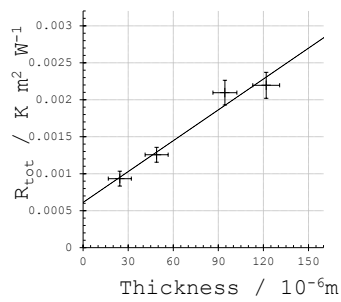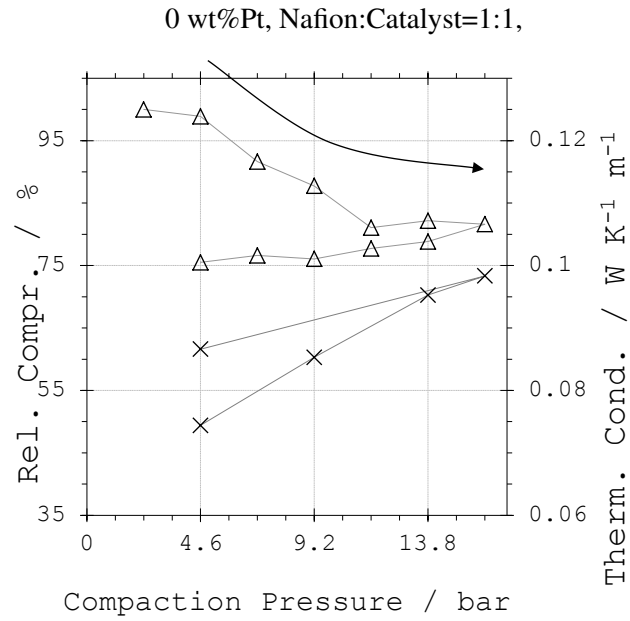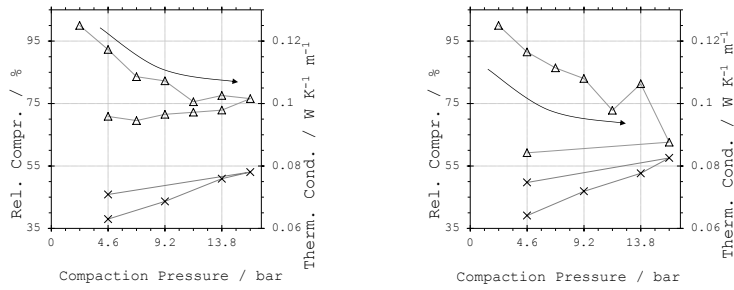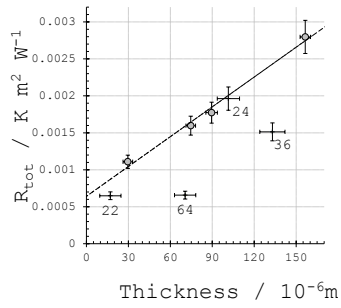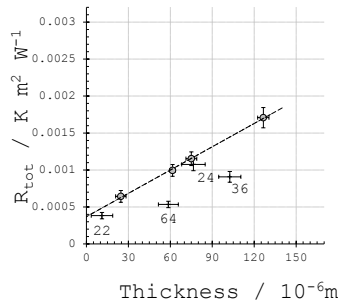
4.6 bar:
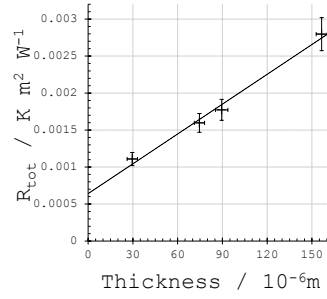
9.3 bar:
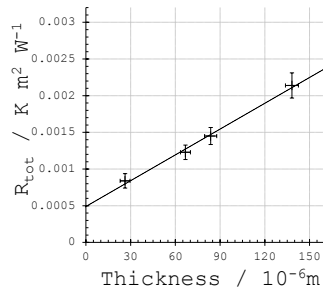
13.8 bar:

16.1 bar:

Figure 4: Measured thermal specific resistance for the CL containing no Pt catalyst and a Nafion®:carbon ratio of 1:1.

Nafion®:Catalyst=1:1

Nafion®:Catalyst=2:1

Figure 5: Measured thermal specific resistance for the CL where the carbon particles contain 20 wt% Pt at a compaction pressure of 9.3 bar.

0 wt%Pt, Nafion:Catalyst=1:1,

20wt%Pt, Nafion®:Catalyst=1:1,   20wt%Pt, Nafion®:Catalyst=2:1,

Figure 6: Measured relative compression (left axes) and thermal conductivity (right axes) from around 4.6 bar compression and upwards to 16.1 bar and down again.
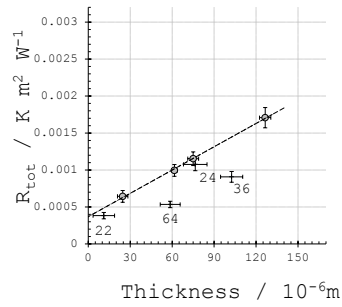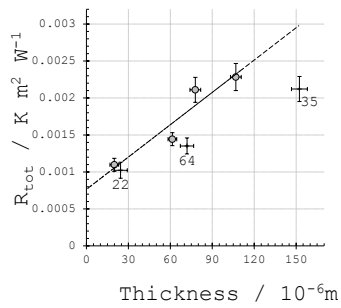
4.6 bar:

9.3 bar:
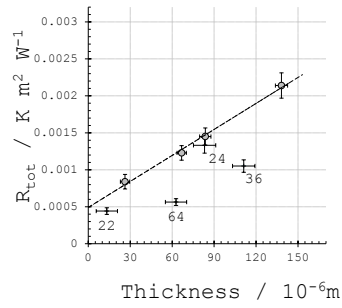
13.8 bar:

16.1 bar:

Figure 7: Measured thermal specific resistance for the CL containing no Pt catalyst and a Nafion®:carbon ratio of 1:1. The figure shows the results for the dry samples and the samples containing water. The water contents, λ, are indicated next to each data point.

Nafion®:catalyst ratio of 1:1

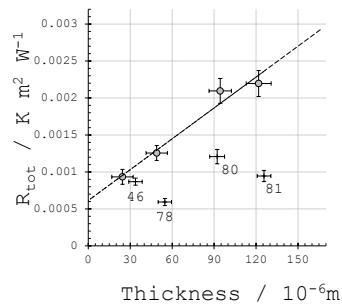Nafion®:catalyst ratio of 2:1:

Figure 8: Measured thermal specific resistance for the humidified CL at 9.3 bar compaction pressure, and with 20 wt%Pt on the carbon and different ionomer content. The water contents, λ, are indicated next to data point.
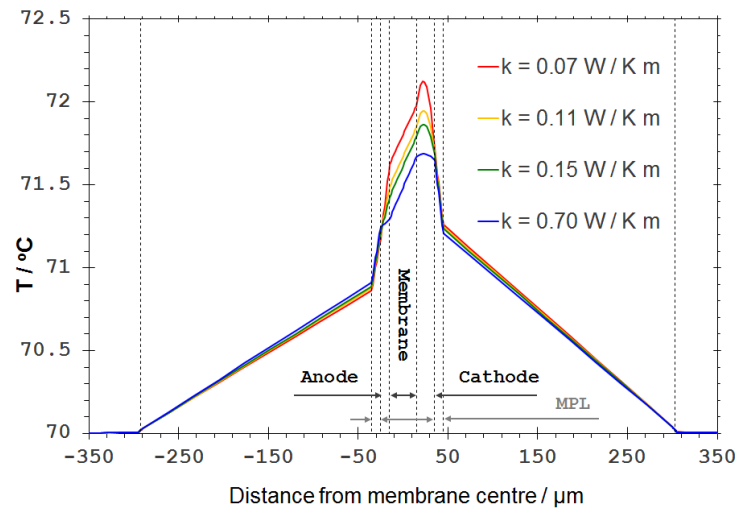
Figure 9: Modeled temperature profiles considered between the middle of two flow channel ribs.